Research Article

# Studies on the utilization of post-distillation liquid from Solvay process to carbon dioxide capture and storage

Natalia Czaplicka[1] · Donata Konopacka-Łyskawa[1]



**Abstract**
In this work, a method of precipitated calcium carbonate production from the post-distillation liquid created in the Solvay process and waste carbon dioxide was proposed and investigated. Precipitation was carried out in a model solution of calcium chloride containing ammonia at various molar ratios in relation to $Ca^{2+}$ ions, while gaseous carbon dioxide was supplied to the reactor as a pure gas or as a mixture with air. It was assumed that the reaction was completed when the pH of the reaction mixture reached the value of 7. To characterize precipitated calcium carbonate particles, its size and crystalline form were determined. It was possible to utilize above 80% of calcium ions from a model post-distillation liquid and above 80% of carbon dioxide from a mixed air-$CO_2$ gas stream using the one-stage precipitation process since the conditions of precipitation were controlled. Calcium carbonate in vaterite form produced in this process can be also a valuable product.

**Keywords** Solvay process · Soda ash · Calcium carbonate · Carbonation · Carbon dioxide

## 1 Introduction

Soda ash (sodium carbonate) is one of the most important substances produced by the chemical industry. It is applied as the second most strategic input raw material, after sand, in the glass industry, and it is used as the main raw material in the detergent and soap production. Soda ash is also necessary for the production of steel and non-ferrous metals. Moreover, it is widely used in the food and pharmacology sectors and in the paper industry, along with flue gas treatment systems and water conditioning and treatment systems. In Europe, due to the availability of raw materials, soda ash is mainly obtained in the Solvay process which was developed by Ernest Solvay in the 1860s [1]. The current worldwide soda ash production performance is estimated to be around 56 million metric ton per year, whereas in Europe combined additional production capacity is 10.7 million metric ton per year [2]. In 2014, 48% of global production of soda ash was produced using the Solvay process, while 27% was obtained by the processing of natural sodium carbonate minerals. The remaining 25% were produced using other methods [2]. Approximately 91% of sodium carbonate is obtained using the Solvay method, regarding Europe [2].

In the Solvay process soda ash is manufactured using the locally available natural raw materials of salt, in the form of brine, limestone and ammonia, as an auxiliary raw material. The process consists of the following main stages: preparation of brine, preparation of the ammonia brine by saturating brine with ammonia, decomposition of limestone to lime and carbon dioxide (Eq. 1), carbonization, i.e., absorption of carbon dioxide in ammonia brine (Eq. 2), separation of crystalline sodium bicarbonate and its calcination (Eq. 3). An important part of this process is the recovery of ammonia from the filter liquid consisting of NaCl and $NH_4Cl$ (Eq. 4). It is treated with lime milk obtained during the process of burning the limestone, and ammonia is released. The evolved

✉ Natalia Czaplicka, natczap1@student.pg.edu.pl | [1]Department of Process Engineering and Chemical Technology, Faculty of Chemistry, Gdansk University of Technology, Narutowicza 11/12, 80-233 Gdańsk, Poland.

SN Applied Sciences (2019) 1:431 | https://doi.org/10.1007/s42452-019-0455-y

Received: 31 January 2019 / Accepted: 4 April 2019

Published online: 08 April 2019

ammonia is vented back into the absorber [3]. Therefore, the whole process is based on the sequence of the following chemical reactions:

$$CaCO_3 \rightarrow CaO + CO_2 \quad (1)$$

$$NaCl + NH_3 + CO_2 + H_2O \rightarrow NaHCO_3 + NH_4Cl. \quad (2)$$

$$2NaHCO_3 \rightarrow Na_2CO_3 + CO_2 \uparrow + H_2O \uparrow \text{ (calcination)} \quad (3)$$

$$2NH_4Cl + CaO \rightarrow 2NH_3 + H_2O + CaCl_2 \quad (4)$$

The main production waste is the post-distillation liquid containing a solid residue consisting mainly of calcium carbonate, unconverted sodium chloride and calcium hydroxide. This liquid flowing out of the stripping columns is directed to ground settlements called "white seas" or straightway to natural water reservoirs [3]. The main components of the post-distillation liquid are water (956 kg/m$^3$ of waste stream), calcium chloride (112 kg/m$^3$) and sodium chloride (56 kg/m$^3$) [3].

The utilization of liquid residue is one of the major problems to be solved in the Solvay technology. Disposal of waste streams in the "white seas" or discharging them directly to surface waters results in a strong salinity of the nearby groundwater with calcium chloride and also contamination of natural water reservoirs and soil [4]. Therefore, it is important to reduce the impact of the post-distillation liquid on the environment.

Another troublesome waste related to many human activities is carbon dioxide. This component of waste gases is generated by energy and chemical plants and accumulates in large amounts in the atmosphere causing dangerous climate changes [5]. Therefore, many efforts are now being made to reduce the amount of $CO_2$ emitted directly into the environment. Various technologies are developed to sequestrate carbon dioxide from gases. Among the conventional $CO_2$ removal methods, the absorption process in which monoethanolamine (abr. MEA) is applied has been extensively studied and it is widely used in chemical plants to post-combustion capture [6]. However, this method involves many problems such as high energy consumption and absorbent degradation by oxygen and acidic compounds present in the gas stream [6, 7]. In addition, there are intensive studies on the use of other amines and their mixtures for efficient post-combustion gas cleaning [8, 9]. As an alternative, an aqueous ammonia solution was proposed as a new absorbent [7, 10]. The main advantage of $NH_3$ is its resistance to oxidative degradation. Therefore, it can be used as an absorbent to treat oxides-containing gas streams, i.e., gas emitted by coal-fired power plants [6]. Also, high $CO_2$ loadings in aqueous ammonia solutions are reported due to the privileged formation of bicarbonate over carbamate in the $CO_2$–$NH_3$–$H_2O$ system for increasing $CO_2$ concentration [11].

In addition, the absorption of $CO_2$ from anthropogenic emissions and its use as a substrate for synthesis of valuable chemicals has gained interest in recent years as an alternative to conventional carbon dioxide capture and storage (CCS) technologies [12]. Attempts have been made to use the post-distillation liquid for the production of gypsum, phosphate and calcium carbonate [1, 3, 11–14]. Recently, carbonation of calcium chloride solution with addition of $CO_2$ absorption promotors, such as amines and ammonia, has been studied in calcium carbonate (PCC) precipitation with the application of desired properties. The overall reaction with ammonia as a $CO_2$ absorption promotor can be written as:

$$CaCl_2 + 2NH_3 + CO_2 + H_2O \rightarrow CaCO_3 \downarrow + 2NH_4Cl \quad (5)$$

In this work, a method for obtaining PCC which allows for the management of the post-distillation liquid from the Solvay process, as well as the use of waste carbon dioxide gas from any source, is proposed. Influence of process parameters such as carbon dioxide concentration in a gas stream supplied into the reaction mixture and the influence of the concentration of ammonia on the efficiency of carbon dioxide sequestration and calcium ion consumption were investigated.

## 2 Experimental

### 2.1 Reagents

Anhydrous calcium chloride (≥ 97.0%, POCH, Gliwice, Poland), sodium chloride (≥ 98.0%, P.P.H. STANLAB, Lublin, Poland), 25% ammonia solution (≥ 96.0%, POCH, Gliwice, Poland). The water used in this work was obtained by reverse osmosis.

### 2.2 Preparation

Precipitation was carried out at room temperature and atmospheric pressure in a glass tank reactor with a total volume of 0.6 dm$^3$ equipped with a magnetic stirrer. The stirring rate was 600 rpm. A solution containing calcium chloride at a concentration of 112 g/dm$^3$, sodium chloride at a concentration of 56 g/dm$^3$ and ammonia in molar ratios of $Ca^{2+}$:$NH_3$ equal to 1:1, 1:1.5 or 1:2 was applied as the reaction mixture in a volume of 0.4 dm$^3$. Carbon dioxide as a pure gas ($X_{V,CO_2} = 1$) or in a mixture with air ($X_{V,CO_2} = 0.15$) was supplied into the liquid phase through a porous glass plate. Gas mixing occurred during the gas flow before it was introduced into the reactor. The gas flow rate was 30 dm$^3$/h in all experiments. During the reaction, the pH of the mixture was measured every 30 s using a ERH-13-6 composite electrode (HYDROMET, Gliwice,

Poland) connected to the pH meter. The process was terminated when the pH of the reaction mixture was equal to 7. The initial and final $Ca^{2+}$ concentrations were determined by a complexometric titration of collected samples ($2 \cdot 10^{-3}$ $dm^3$) with EDTA. Obtained calcium carbonate suspension was filtered, washed with water and methanol, and then dried at 90 °C. The scheme of the reaction setup used to carry out the precipitation is presented in Fig. 1.

### 2.3 Characterization of particles

Fourier transform infrared spectroscopy (ATR FT-IR) was applied using the Nicolet 8700 Spectrometer (Thermo Scientific) to identify the types of chemical bonds in structural units of the obtained calcium carbonate particles. The method of suppressed total reflection (ATR) was used. The infrared spectra were registered from 4500 to 524 $cm^{-1}$ at 2 $cm^{-1}$ resolution using air as the background. To characterize polymorphic composition of precipitated particles, conventional XRD technique with Co $K_\alpha$ radiation using the MiniFlex 600 diffractometer (Rigaku) was carried out. The XRD spectra were collected at a scan rate 0.01° and $2\theta$ angle range of 10°–80° at room temperature. Obtained particles were observed by a BX60 microscope (Olympus) equipped with a digital camera XC50 (Olympus), and the effective magnification used was equal to 1000×.

## 3 Results and discussion

### 3.1 Course of reaction

During the precipitation of calcium carbonate, pH of reaction mixture was monitored. Figure 2 presents courses of pH versus time for a different composition of gas supplied into the reaction mixture and for various ammonia concentration. In case of pure carbon dioxide application, the reaction time was shorter for every applied $Ca^{2+}$:$NH_3$ molar ratios compared to supplying the mixture of $CO_2$ and air. However, regardless of the composition of gas introduced into the system, the solution pH of 7 was reached in the shortest time by the molar ratio of 1:1, while for the 1:2 ratio the pH stabilization time was the longest. Thus, it can be concluded

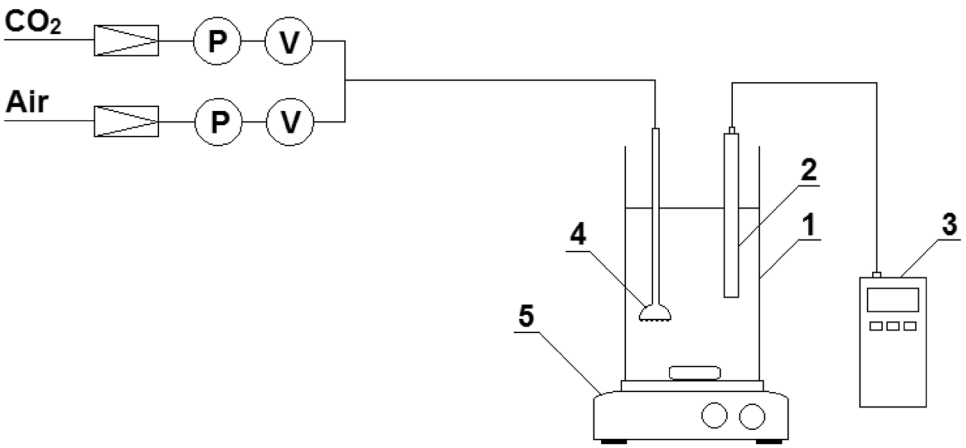


**Fig. 1** Scheme of the experimental setup: 1—glass tank reactor, 2—pH electrode, 3—pH meter, 4—gas distributor, 5—magnetic stirrer, P—manometer, V—rotameter

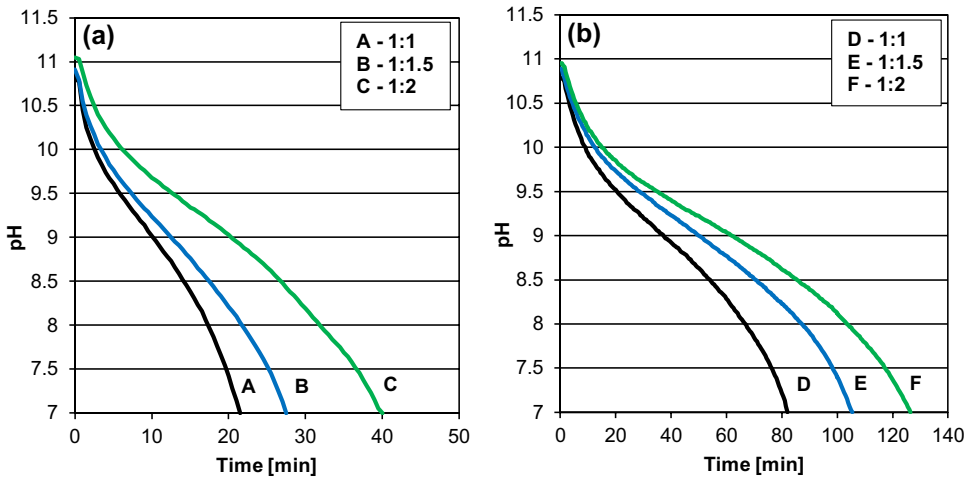


**Fig. 2** pH values of reaction mixture versus time for $X_{V,CO_2} = 1$ (**a**) and 0.15 (**b**) depending on the ammonia concentration

**Table 1** Reaction time, initial and final concentrations of calcium ions

| Process ID | $X_{V,CO_2}$ | $Ca^{2+}$:$NH_3$ molar ratio | Reaction time (min) | $Ca^{2+}$ concentration (mol/dm$^3$) | |
|---|---|---|---|---|---|
| | | | | Initial ($C_i$) | Final ($C_f$) |
| A | 1 | 1:1 | 21.5 | 1.01 | 0.54 |
| B | | 1:1.5 | 27.5 | 1.01 | 0.43 |
| C | | 1:2 | 40 | 1.01 | 0.38 |
| D | 0.15 | 1:1 | 82 | 1.01 | 0.55 |
| E | | 1:1.5 | 105.5 | 1.01 | 0.48 |
| F | | 1:2 | 126.5 | 1.01 | 0.20 |

**Table 2** Sequestration of $Ca^{2+}$ and $CO_2$, percentage content of vaterite and mean sizes of crystallites forming PCC particles

| Sample ID | %$Ca^{2+}$ | %$CO_2$ | $X_V$ (%) | $D$ (nm) |
|---|---|---|---|---|
| A | 46.4 | 42.2 | 97.4 | 26 |
| B | 57.3 | 40.8 | 99.1 | 26 |
| C | 62.1 | 30.4 | 98.9 | 22 |
| D | 45.9 | 73.1 | 96.3 | 25 |
| E | 52.6 | 65.0 | 97.7 | 19 |
| F | 80.1 | 82.6 | 99.2 | 19 |

that an increase in the ammonia content in the reaction mixture results in an increase in the reaction time.

Table 1 summarizes reaction time, initial and final concentrations of $Ca^{2+}$ depending on the process parameters.

Based on the reaction conditions and data presented in Table 2, the amount of consumed $Ca^{2+}$ ions and the amount of $CO_2$ supplied to the system during the reaction were calculated. Then, the sequestrations of calcium ions %Ca and carbon dioxide %$CO_2$ were determined using the following equations:

$$\%Ca^{2+} = \frac{C_i - C_f}{C_i} \cdot 100\% \quad (6)$$

$$\%CO_2 = \frac{n_{CaCO_3}}{n_{CO_2}} \cdot 100\% \quad (7)$$

where $C_i$ and $C_i$ are initial and final $Ca^{2+}$ concentration, $n_{CaCO_3}$ and $n_{CO_2}$ are the number of $CaCO_3$ mol corresponding to the number of $CO_2$ mol consumed during precipitation and the number of $CO_2$ mol supplied into the reaction system, respectively. All calculated values for studied processes are summarized in Table 2. The sequestration of calcium ions increases with an increase in ammonia concentration in the reaction mixture, regardless of $CO_2$ content in supplied gas. When pure carbon dioxide is introduced, $CO_2$ sequestration decreases with an increase in ammonia concentration, while for D-F (see Table 1) processes carried out using a gas mixture, such relationship is not observed. The highest percentage of sequestration of both, $Ca^{2+}$ ions and $CO_2$, was achieved during F process, which was characterized by the longest duration.

The mechanisms of $CO_2$ absorption into an aqueous ammonia solution include a very fast formation of carbamic acid during the chemical reaction between ammonia and $CO_2$(aq) (which deprotonates to carbamate). Consequently carbamate decomposes to ammonium and bicarbonate ions [15]. Due to the bicarbonate–carbonate equilibrium, the reaction leading to the formation of calcium carbonate occurs. The rate of $CO_2$ absorption in ammonia solutions depends on the ammonia concentration and the partial pressure of carbon dioxide [16]. The higher the $CO_2$ partial pressure and ammonia concentration, the higher the $CO_2$ absorption flux. Therefore, the time related to the ammonia concentration decreases with an increase in $NH_3$ contents in the reaction mixture and decreases with an increase in $CO_2$ volume fraction in the gas stream.

However, consumption of both calcium ions and carbon dioxide depends on the calcium carbonate formation. Two main stages in the precipitation process are distinguished, i.e., nucleation and crystal growth, and in addition, secondary processes such as agglomeration or attrition of formed crystals. Nucleation precedes the induction period that is needed to create the supersaturation in the solution, pre-nucleation clusters, and then consequently the critical nuclei. The supersaturation in the reactive mixture is a result of $CO_2$ absorption. Therefore, some volume of $CO_2$ should be supplied into the solution to start the precipitation process. Estimated induction period was evaluated on the basis of both visual observation of the reactive mixture and the analysis of $Ca^{2+}$ ions concentration in the filtrated samples. In case of all processes with pure $CO_2$, the induction time was lower than 2 min, while for processes with application of gas mixture the induction time was in the range of 4–8 min.

### 3.2 Particles characteristic

PCC particles were analyzed by ATR FT-IR and XRD. Figure 3 presents the FT-IR spectra of obtained particles in range of 700–800 cm$^{-1}$. The shown excerpt of spectrum is the fingerprint region in which the bands corresponding to the plane bending oscillations originating from C–O bond are observed. In all spectra, wide bands at wave number of 745 cm$^{-1}$ are visible, which is characteristic for vaterite.

XRD patterns of obtained PCC particles are shown in Fig. 4 in 2$\theta$ range of 10°–80°.

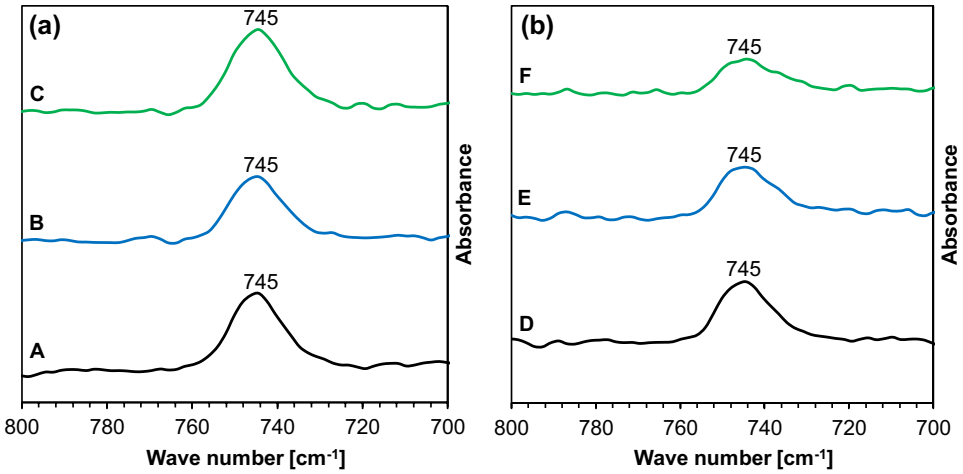


**Fig. 3** FT-IR spectra of obtained $CaCO_3$ particles produced using a pure $CO_2$ (**a**) and a mixture $CO_2$—air $X_{V,CO_2}=0.15$ (**b**) depending on the ammonia concentration

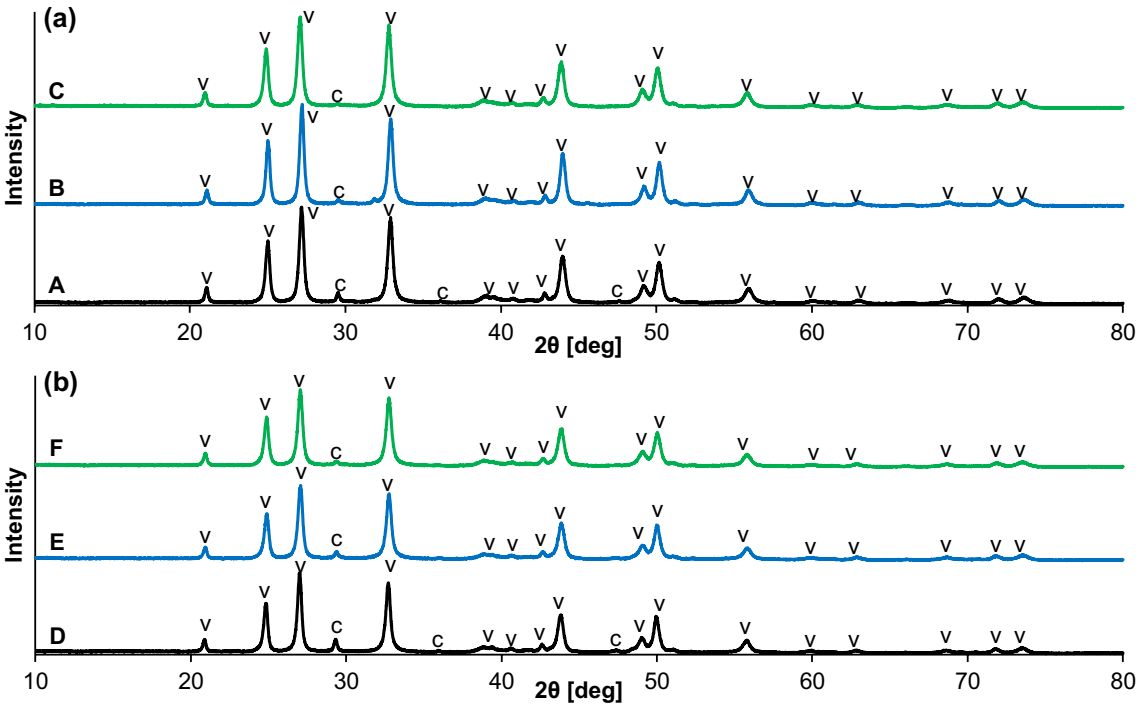


**Fig. 4** XRD patterns of obtained $CaCO_3$ particles produced using a pure $CO_2$ (**a**) and a mixture $CO_2$—air $X_{V,CO_2}=0.15$ (**b**) depending on the ammonia concentration (*c* calcite, *v* vaterite)

The percentage content of vaterite ($X_V$) was calculated based on the XRD data, using the equations [17, 18]:

$$X_V = \frac{7.691\left(I_V^{110}\right)}{I_C^{104} + 7.691\left(I_V^{110}\right)} \quad (8)$$

where $I_C^{104}$ is the intensity of the calcite peak of the 104 plane and the $I_V^{110}$ is the intensity of the vaterite peak of the 110 plane. Calculated percentage contents of vaterite in tested samples are summarized in Table 2. As a result of each reaction calcium carbonate as a mixture of vaterite and calcite was formed, however the main polymorph form was vaterite. The results in Table 2 show that for each case PCC consisted of more than 95% of vaterite. The least calcite was found in the sample F obtained with the application of a gas-air mixture and the highest concentration of ammonia, whereas calcium carbonate precipitated with the supply of a gas mixture and in the presence of the lowest $NH_3$ concentration (sample D) was characterized by the lowest content of vaterite.

Based on XRD measurements, the mean size of crystallites ($D$) forming calcium carbonate particles was also determined. The Scherrer equation was used for this purpose [19]:

$$D = \frac{K\lambda}{B\cos\theta_B} \quad (9)$$

where $K$ is a Scherrer constant (0.89), $\lambda$ is the X-ray wavelength, $B$ is the width of the diffraction line measured at half the high of the peak, and $\theta_B$ is the Bragg angle. Calculated mean sizes of crystallites are presented in Table 2. Crystallites forming samples A and B had similar mean size, which occurred as the largest of all measured samples. Only in case of precipitation with supplying gas mixture to the system using higher ammonia concentrations (samples E and F) crystallites with an average size of 19 nm were obtained.

Microscope photographs of the obtained PCC particles are shown in Fig. 5. The precipitated particles are characterized by a size below 5 µm.

The calcium carbonate polymorph formation depends on such parameters as supersaturation, pH, temperature, the concentration of reagents, duration of the reaction and the presence of various inorganic and organic additives [20, 21]. In our experiments mainly vaterite particles were generated. This polymorph is less stable, and its formation is favored by prevailing local high saturation determined by a slightly alkaline pH, which inhibits the transformation of vaterite into calcite [22, 23]. According to Takita et al. [24] the presence of NaCl in the solution increases the solubility of calcium carbonate. Therefore, the lower supersaturation occurs in the system and the formation of calcite form should be expected. On the other hand, the presence of carbamate ions formed during $CO_2$ absorption in the ammonia solution can stabilize vaterite form [23].

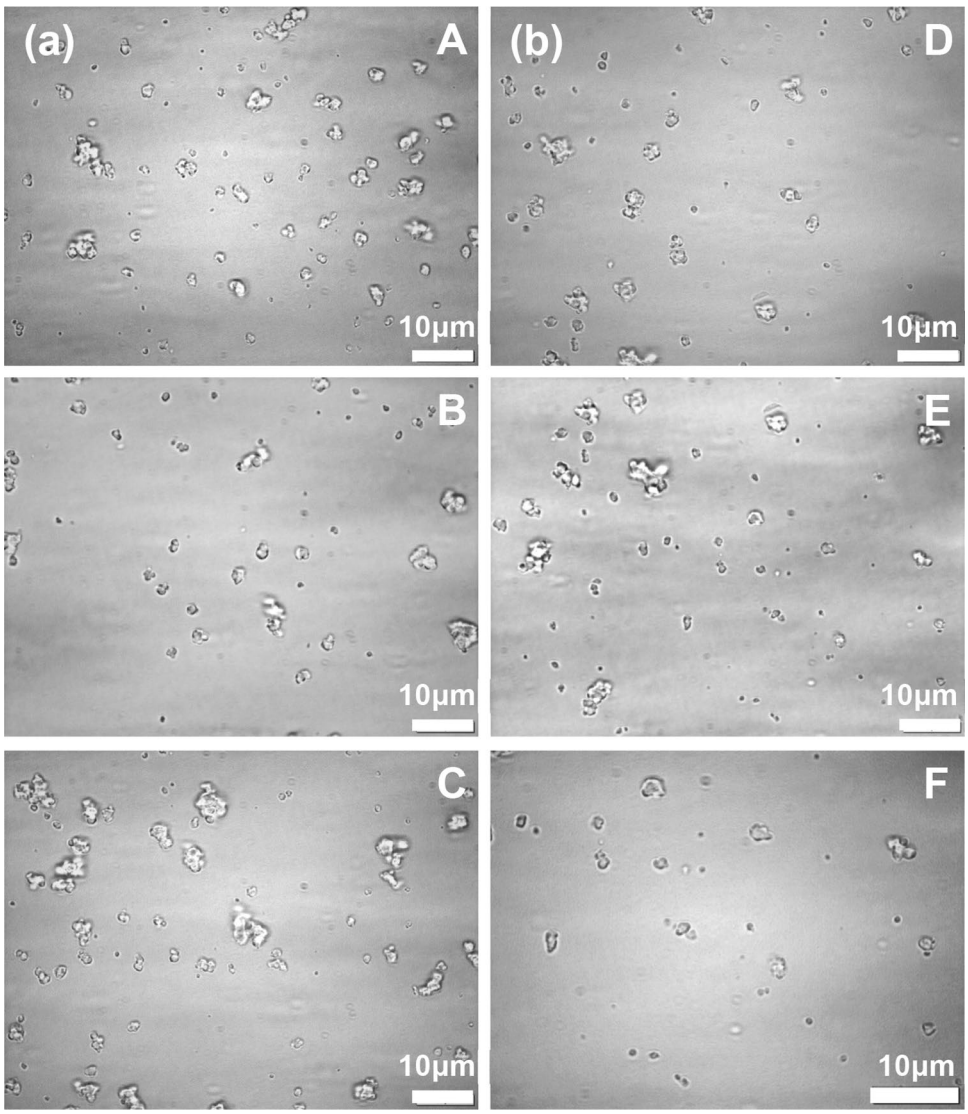


**Fig. 5** Microscope photographs of PCC particles produced using a pure $CO_2$ (**a**) and a mixture $CO_2$—air $X_{V,CO_2} = 0.15$ (**b**) depending on the ammonia concentration

Vaterite, thanks to its porous structure, with a larger surface area and a greater hydrophilicity than other polymorphic phases, is used to create new materials with promising perspectives in various fields [25]. Spherical particles of vaterite can efficiently replace silica in the coating pigments, and they are also used in the production of paper. In addition, vaterite is used as a filler in polymeric composites, as it improves the degree of crystallinity, the crystallization temperature and the size of the composite spherulites [22]. The application of vaterite as an adsorbent for heavy metal ions removal is also examined [26]. Therefore, calcium carbonate in vaterite form can be a valuable by-product in the proposed process. During the proposed $CaCO_3$ precipitation process described by Eq. (5), a solution containing ammonium chloride is also produced. This solution can be used as a leaching agent to treat a steelmaking slag [27], some minerals [28] or batteries [29, 30] and for metal ions recovery. The obtained leachates can be used in a carbon capture and storage process [31] or it can be further processed [30].

## 4 Conclusions

The method using the post-distillation liquid form the Solvay process for carbon dioxide sequestration was proposed. The highest efficiency of carbon dioxide capture was obtained for the $CO_2$ concentration in a gas stream corresponding to the composition of exhausted gases produced by the fossil fuels combustion. An increase in the ratio of ammonia to calcium ions favored carbon dioxide and calcium ions consumption during this process. Fine calcium carbonate particles in vaterite form were produced in all experiments. The investigations were carried out with the use of model solutions; therefore, the next step will be to carry out experiments with the waste solution from soda production using the Solvay method to verify and optimize the proposed method.

**Acknowledgements** The authors would like to thank colleagues from Gdansk University of Technology (Poland), from the Department of Process Engineering and Chemical Technology for their help in the XRD analysis. Special thanks go to Dr P. Bruździak from Department of Physical Chemistry for enabling FT-IR analyzes and to Dr M. Serocki from Department of Pharmaceutical Technology and Biochemistry for providing equipment and assistance in taking microscopic photographs.

**Funding** This work was financially supported by the Faculty of Chemistry, Gdansk University of Technology, Poland (Grant No. DS 033155).

### Compliance with ethical standards

**Conflict of interest** The authors declare that they have no conflict of interest.



## References

1. Steinhauser G (2008) Cleaner production in the Solvay Process: general strategies and recent developments. J Clean Prod 16:833–841
2. SOLVAY Clemente Ch (2018) Soda ash & derivatives resilient cash generator for Solvay. https://vdocuments.mx/soda-ash-derivatives-resilient-cash-generator-for-solvay.html. Accessed 10 Dec 2018
3. Kasikowski T, Buczkowski R, Lemanowska E (2004) Cleaner production in the ammonia-soda industry: an ecological and economic study. J Environ Manag 73:339–356
4. Hulisz P, Piernik A (2013) Soils affected by soda industry in Inowrocław. In: Charzyński P, Hulisz P, Bednarek R (eds) Technologenic soils of Poland. Polish Society of Soil Science, Toruń, pp 125–140
5. Sha F, Zhu N, Bai Y, Li Q, Guo B, Zhao T, Zhang F, Zhang J (2016) Controllable synthesis of various $CaCO_3$ morphologies based on a CCUS idea. ACS Sustain Chem Eng 4:3032–3044
6. Puxty G, Rowland R, Attalla M (2010) Comparison of the rate of $CO_2$ absorption into aqueous ammonia and monoethanolamine. Chem Eng Sci 65:915–922
7. Luis P (2016) Use of monoethanolamine (MEA) for $CO_2$ capture in a global scenario: consequences and alternatives. Desalination 380:93–99
8. Puxty G, Rowland R, Allport A, Yang Q, Bown M, Burns R, Maeder M, Attalla M (2009) Carbon dioxide postcombustion capture: a novel screening study of the carbon dioxide absorption performance of 76 amines. Environ Sci Technol 43:6427–6433
9. Bougie F, Iliuta MC (2010) Analysis of regeneration of sterically hindered alkanolamines aqueous solutions with and without activator. Chem Eng Sci 65:4746–4750
10. Budzianowski WM (2011) $CO_2$ reactive absorption from flue gases into aqueous ammonia solutions: the $NH_3$ slippage effect. Environ Prot Eng 37:5–19
11. Mani F, Peruzzini M, Stoppioni P (2006) $CO_2$ absorption by aqueous $NH_3$ solutions: speciation of ammonium carbamate, bicarbonate and carbonate by 13C NMR study. Green Chem 8:995–1000
12. Barzagli F, Giorgi C, Mani F, Peruzzini M (2017) $CO_2$ capture by aqueous $Na_2CO_3$ integrated with high-quality $CaCO_3$ formation and pure $CO_2$ release at room conditions. J CO2 Util 22:346–354
13. Trypuć M, Białowicz K (2011) $CaCO_3$ production using liquid waste from Solvay method. J Clean Prod 19:751–756
14. Gao C, Dong Y, Zhang H, Zhang J (2007) Utilization of distiller waste and residual mother liquor to prepare precipitated calcium carbonate. J Clean Prod 15:1419–1425
15. Wang X, Conway W, Fernandes D, Lawrance G, Burns R, Puxty G, Maeder M (2011) Kinetics of the reversible reaction of $CO_2$(aq) with ammonia in aqueous solution. J Phys Chem 115:6405–6412
16. Puxty G, Rowland R, Attalla M (2010) Comparison of the rate of $CO_2$ absorption into aqueous ammonia and monoethanolamine. Chem Eng Sci 65:915–922
17. Kontoyannis CG, Vagenas NV (2000) Calcium carbonate phase analysis using XRD and FT-Raman spectroscopy. Analyst 125:251–255

18. Konopacka-Łyskawa D, Kościelska B, Karczewski J, Gołębiewska A (2017) The influence of ammonia and selected amines on the characteristics of calcium carbonate precipitated from calcium chloride solutions via carbonation. Mat Chem Phys 193:13–18
19. Tran HV, Tran LD, Vu HD, Thai H (2010) Facile surface modification of nanoprecipitated calcium carbonate by adsorption of sodium stearate in aqueous solution. Colloid Surf A 366(1–3):95–103
20. Kitamura M (2002) Controlling factor of polymorphism in crystallization process. J Cryst Growth 237–239:2205–2214
21. Kędra-Królik K, Gierycz P (2006) Obtaining calcium carbonate in a multhiphase system by the use of new rotating disc precipitation reactor. J Therm Anal Calorim 83:579–582
22. Udrea I, Capat C, Olaru EA, Isopescu R, Mihai M, Mateescu CD, Bradu C (2012) Vaterite synthesis via gas-liquid route under controlled pH conditions. Ind Eng Chem Res 52:8185–8193
23. Popescu MA, Isopescu R, Matei C, Fagarasan G, Plesu V (2014) Thermal decomposition of calcium carbonate polymorphs precipitated in the presence of ammonia and alkylamines. Adv Powder Technol 25:500–507
24. Takita Y, Eto M, Sugihara H, Nagaoka K (2007) Promotion mechanism of co-existing NaCl in the synthesis of $CaCO_3$. Mater Lett 61:3083–3085
25. Boyjoo Y, Pareek VK, Liu J (2014) Synthesis of micro and nano-sized calcium carbonate particles and their applications. J Mater Chem A 2:14270–14288
26. Dang HC, Yuan X, Xiao Q, Xiao WX, Luo YK, Wang XL, Song F, Wang YZ (2017) Facile batch synthesis of porous vaterite microspheres for high efficient and fast removal of toxic heavy metal ions. J Environ Chem Eng 5:4505–4515
27. Hall C, Large DJ, Adderley B, West HM (2014) Calcium leaching from waste steelmaking slag: significance of leachate chemistry and effects on slag grain mineralogy. Miner Eng 65:156–162
28. Li J, Li D, Xu Z, Liao C, Liu Y, Zhong B (2018) Selective leaching of valuable metals from laterite nickel ore with ammonium chloride-hydrochloric acid solution. J Clean Prod 179:24–30
29. Lv W, Wang Z, Cao H, Zheng X, Jin W, Zhang Y, Sun Z (2018) A sustainable process for metal recycling from spent lithium-ion batteries using ammonium chloride. Waste Manag 79:545–553
30. Kuzharov AS, Lipkin MS, Kuzharov AA, Lipkin VM, Nguen K, Shishka VG, Rybalko EA, Lytkin NA, Misharev AS, Tulaeva FR, Gaidar AI (2015) Green tribology: disposal and recycling of waste Ni–Cd batteries to produce functional tribological materials. J Frict Wear 4:306–3013
31. Sun Y, Yao M-S, Zhang J-P, Yang G (2011) Indirect $CO_2$ mineral sequestration by steelmaking slag with $NH_4Cl$ as leaching solution. Chem Eng J 173:437–445